

19. CLIMATE CHANGE INCREASED THE LIKELIHOOD OF THE 2016 HEAT EXTREMES IN ASIA

YUKIKO IMADA, HIDEO SHIOGAMA, CHIHARU TAKAHASHI, MASAHIRO WATANABE,
MASATO MORI, YOUICHI KAMAE, AND SHUHEI MAEDA

The 2016 extreme warmth across Asia would not have been possible without climate change. The 2015/16 El Niño also contributed to regional warm extremes over Southeast Asia and the Maritime Continent.

Introduction. Analyses of the observed monthly temperature record from the Goddard Institute for Space Studies (GISS) Surface Temperature Analysis (GISTEMP; Hansen et al. 2010) indicate that the total area that experienced extreme warmth over the global land surface in 2016 was record-breaking, exceeding the previous highest record in 2010 (Fig. 19.1a, fraction of area that experiences extremely high temperature). This frequent occurrence of warm events is particularly remarkable over the Asian region (Fig. 19.1a). Many parts of Southeast Asia, southern India, and northern Eurasia experienced extremely high temperature by the end of 2016 (Fig. 19.1b). In India, at least 580 people were killed by the heat waves from March to May (India's government; European Commission). The record-breaking high temperature had been persistent more than 10 months in the Maritime Continent. In Thailand, the heat wave also caused a new record for energy consumption because of the nationwide usage of air conditioners (Gecker and Chuwiruch 2016).

Generally, Southeast Asia experiences warm and dry conditions during El Niño, being in the region of anomalously downward motion associated with the weakened Walker Circulation. Also, the global surface warms up with a lag of several months following

an El Niño event through persistent changes in atmospheric circulation (Trenberth et al. 2002). In this report, we investigate to what extent the 2016 extreme warmth across Asia was attributable to anthropogenic warming or to the major El Niño episode in 2015/16.

Many studies have concluded that heat waves over the global land area have become more frequent due to human-induced global warming (e.g., Jones et al. 2008; Christidis and Stott 2014; Shiogama et al. 2016). To separate the influences of anthropogenic warming and natural variability on the 2016 heat events in Asia, we analyzed large ensembles of atmospheric general circulation model (AGCM) simulations with and without anthropogenic warming and ENSO effects.

Methods. We performed several 100-member ensemble experiments of 2016 (initialized on 1 June 2009 and continuously updated every year) using the AGCM of MIROC5 (T85L40, Watanabe et al. 2010): 1) ALL: All-forcing run integrated by the historical sea surface temperature (SST) and sea ice (HadISST dataset, Rayner et al. 2003) and historical anthropogenic and natural forcing agents. 2) NAT1 and NAT2: Natural forcing runs by removing 1870–2012 linear trends of the observed SST and sea ice (NAT1, Christidis and Stott 2014), and by removing the estimates of anthropogenic changes in SST and sea ice based on the Coupled Model Intercomparison Project Phase 5 (CMIP5) historical experiments (NAT2, Stone 2013). See Shiogama et al. (2014) for details of ALL and NAT. 3) ALLnoENSO: Same as ALL but ENSO-related variability was eliminated by removing the observed SST anomaly regressed to the Niño-3.4 SST anomaly (Takahashi et al. 2016) in order to examine the impact of the extreme El Niño in 2015/16. The SST patterns removed in NAT1, NAT2, and ALLnoENSO are shown in Figure ES19.1. The long-term historical run, ALL-LNG (1949–2016), which also uses observed SST and sea ice as specified forcings, is also

AFFILIATIONS: IMADA—Meteorological Research Institute, Japan Meteorological Agency, Ibaraki, Japan; SHIOGAMA—Center for Global Environmental Research, National Institute for Environmental Studies, Ibaraki, Japan; TAKAHASHI AND WATANABE—Atmosphere and Ocean Research Institute, University of Tokyo, Chiba, Japan; MORI—Research Center for Advanced Science and Technology, University of Tokyo, Tokyo, Japan; KAMAE—Faculty of Life and Environmental Sciences, University of Tsukuba, Ibaraki, Japan, and Scripps Institution of Oceanography, University of California, San Diego, California; MAEDA—Japan Meteorological Agency, Tokyo, Japan

DOI:10.1175/BAMS-D-17-0109.1

A supplement to this article is available online (10.1175/BAMS-D-16-0109.2)

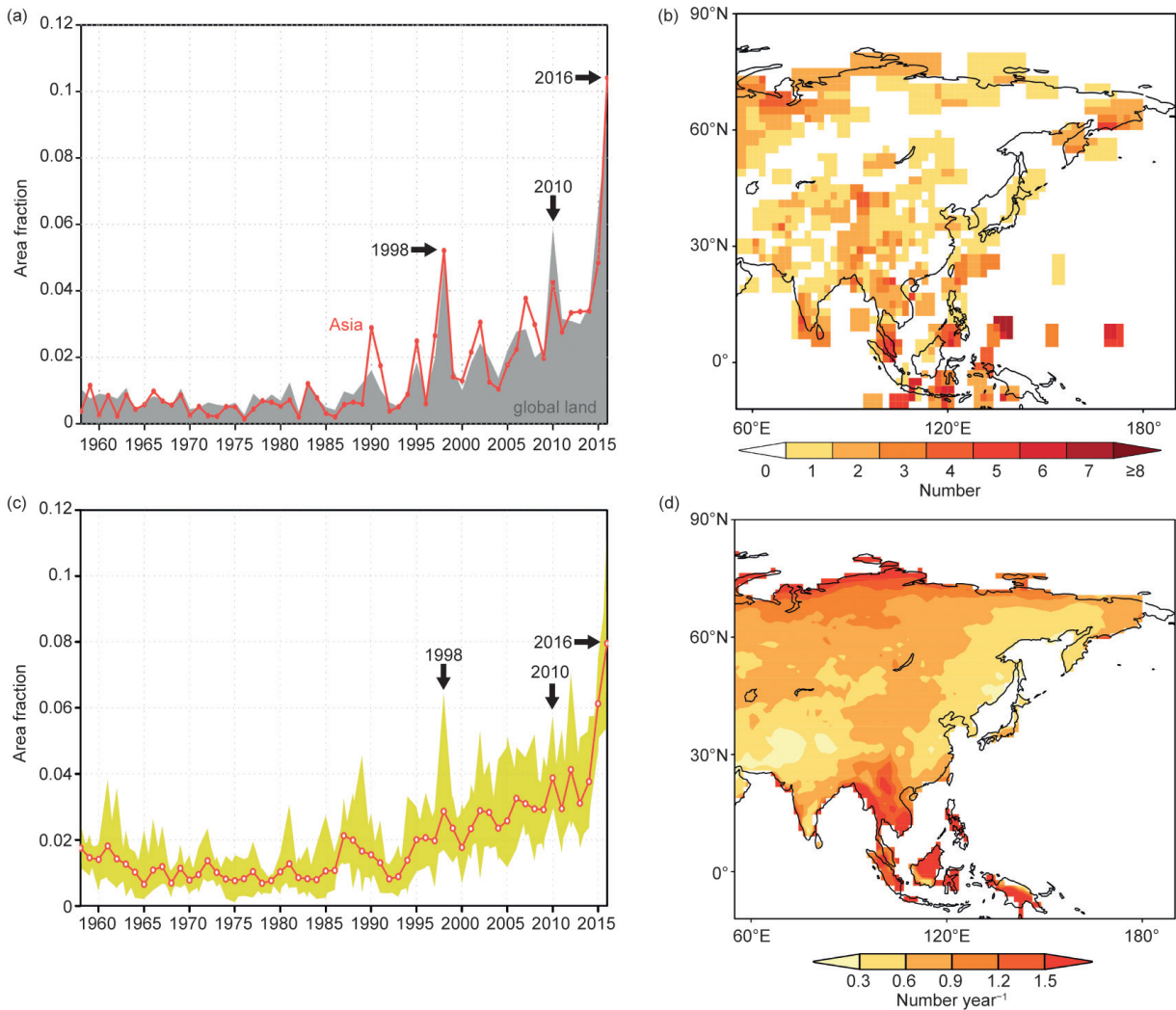


FIG. 19.1. (a) Time series of area fraction with extreme warmth, defined as total land surface area with extreme warmth (exceeding 2 std. dev.) divided by total area of available grid points, based on GISTEMP dataset. Global land surface (gray shaded) and Asian region (10°S–90°N, 55°E–170°W) (red) are shown. (b) Map of number of monthly warm events in 2016. (c) Same as Asian time series of (a) but ensemble mean values (red line) and range (shaded) of 10 member simulations of ALL-LNG are shown. (d) Same as (b) but for result from 2016 ensemble simulations of ALL, where number of monthly warm events was divided by 100 (number of members) to get annual value number per year. Values exceeding 99% confidential level by Student’s t test are plotted.

conducted with 10-member ensembles for validation and to define a threshold of warm events. We used the monthly observation data from GISTEMP for land surface temperature.

For each land–surface grid point, annual time series of the total number of months exceeding a threshold are calculated. The thresholds for the observation and simulations are defined by two standard deviations of surface air temperature from 1951 to 2016 for GISTEMP and ALL-LNG, respectively. We assessed relative contributions of human influence and ENSO to the frequent occurrences of extreme warmth in terms of the fraction of attributable risk

(FAR; Allen 2003), defined as $1 - (P_0 / P_1)$, where P_1 and P_0 are threshold exceedances computed with the ALL and NAT/ALLnoENSO simulations, respectively. The threshold is defined as a 99-percentile value of area fraction estimated by the kernel method (Silverman 1986; Kimoto and Ghil 1993); 0.103 for the observation and 0.065 for the simulations (the ALL-LNG simulation underestimates the extreme values of the area fraction).

Results. Figure 19.1c depicts the modeled time series of the fraction: area-weighted total number of grid points experiencing extremely high temperature

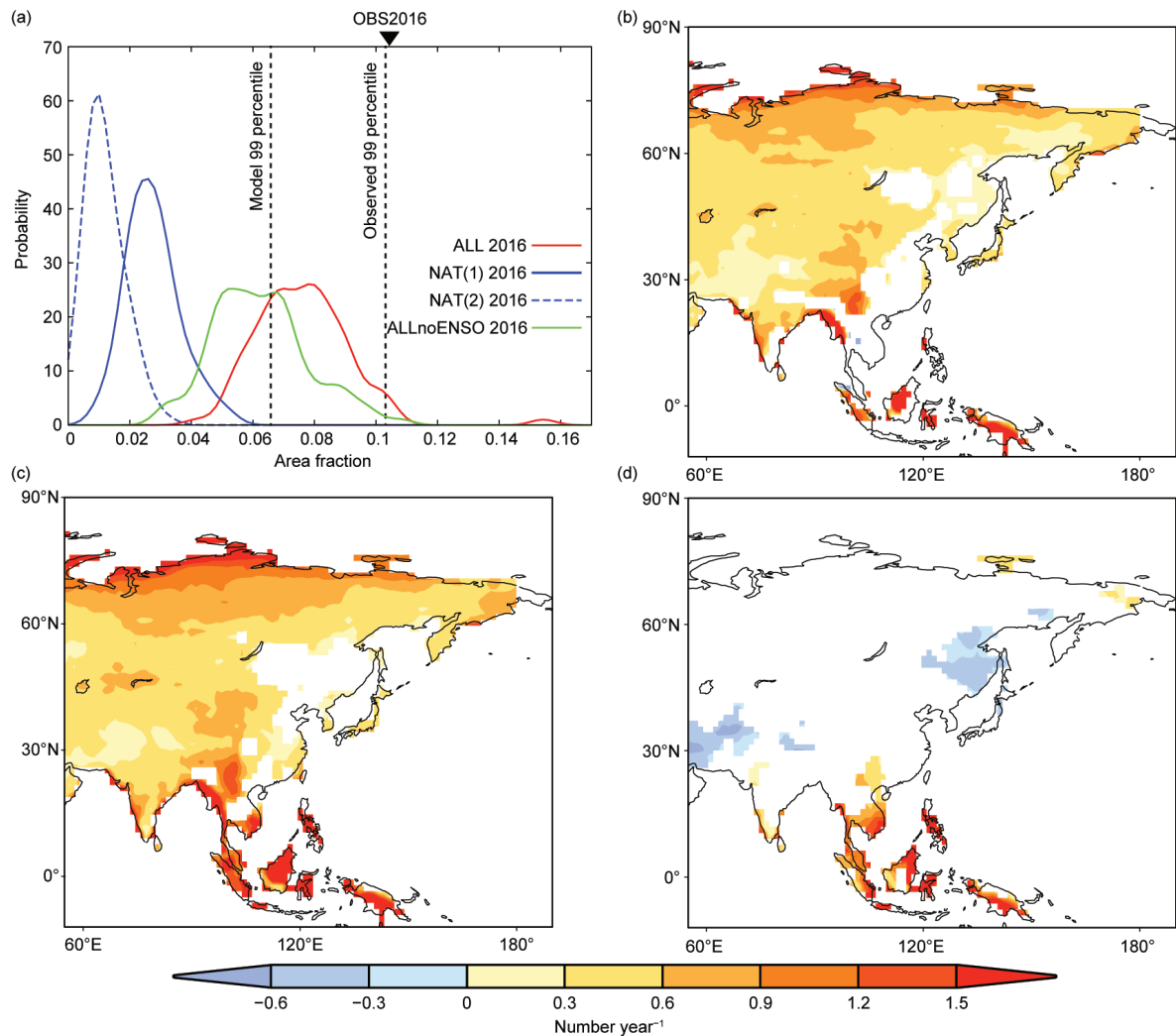


FIG. 19.2. (a) PDFs of annual area fraction of extreme warmth over Asian region in 2016 for ALL (red), NAT1 (blue, solid), NAT2 (blue, broken), and ALLnoENSO (green) estimated by kernel method (Silverman 1986; Kitamoto and Ghil 1993). (b) Map of difference in frequency of extreme warmth (per year) between ALL and NAT1 (ALL minus NAT1). Extreme warmth is defined as monthly temperatures that exceed 2 std. dev. of 1951–2016 average. (c), (d) Same as (b) but for ALL minus NAT2 and ALL minus ALLnoENSO, respectively. In (b)–(d), values exceeding 99% confidential level by Student’s *t* test are plotted.

divided by the total number of available grid points (hereinafter, referred to as “area fraction”) over the Asian region from the ALL-LNG runs. The ALL-LNG model captures peaks of the area fraction occurring after large El Niño events (1998, 2010, and 2016) and the most frequent occurrence of warmth in 2016 (Fig. 19.1c). The model also captures the general trend of the observations. Owing to the large ensembles, a simulated event frequency map based on the 100-member ALL simulations (Fig. 19.1d) depicts continuous distribution, and reproduces the concentration of the events in Southeast Asia, southern India, and northern Eurasia.

Next, we constructed probability density functions (PDFs) of the area fraction of extreme warmth over

the Asian region in 2016 using the ALL, NAT1, NAT2, and ALLnoENSO simulations (Fig. 19.2a). The results indicate that anthropogenic forcing leads to a marked increase in the event occurrence although there is a certain degree of uncertainty induced by the different estimations of anthropogenic changes in SST and sea ice between NAT1 and NAT2. Compared with this, the impact of ENSO is weaker but substantially increases the area fraction of extreme warmth.

The effects of the anthropogenic warming and ENSO on the occurrence of extreme warmth are evaluated from the difference between ALL and NAT, and ALL and ALLnoENSO, respectively. Again, extreme warmth months are defined as monthly temperatures that exceed 2 standard deviations of

the 1951–2016 average from the ALL-LNG run. The spatial maps of frequency change due to anthropogenic forcing (Figs. 19.2b,c) indicate that the frequent occurrence of warm events across Asia shown in Fig. 19.1d can be attributable to the anthropogenic effect in most regions except narrow parts of East Asia and the Indochina peninsula. On the other hand, the ENSO-induced frequency change (Fig. 19.2d) shows increased incidence particularly over Southeast Asia. The positive frequency anomalies of extreme warmth over Southeast Asia appeared during the months from January to May in 2016 (not shown) and seem to be attributable to the warmer Indian Ocean SSTs and descending anomalies over the Maritime Continent during that period associated with the continued big El Niño since the 2015 winter (the ENSO-related SST transition in 2016 is shown in Fig. ES19.1c). Note that, in our simple concurrent regression method, lagged influence of ENSO on the East Asian summer climate (the so-called Indian Ocean capacitor effect; Xie et al. 2009, 2016) cannot be taken into account. In 2016, however, the major Indian Ocean warming occurred in the beginning of the year, which is partly captured in the concurrent regression method (Fig. ES19.1c), and the lagged impact of ENSO was relatively small in the summer.

From the observed record, the occurrence rate of extreme area fraction in 2016 can be estimated at less than 1% in the long-term climate (the observed area fraction of 2016 is greater than the 99-percentile threshold). The ALL simulations, however, indicate that the 2016 condition raised the level of the occurrence rate up to 75.9%. On the other hand, the occurrence rate is 0.000%, 0.000%, and 41.1% for NAT1, NAT2, and ALLnoENSO, respectively. The estimated FARs are 1.000, 1.000, and 0.458, respectively. These results suggest that the frequent occurrence of extreme warmth across Asia in 2016 would never have happened without the anthropogenic warming, and the ENSO condition also partly contributed to the increase in the probability particularly over the Philippines, the Maritime Continent, and Southeast Asia.

Several studies demonstrated that the magnitude of the attributable signal can change substantially depending on the model used (e.g., Bellprat and Doblas-Reyes 2016). It is also known that the atmosphere-only model experiments lack air–sea interactions and overestimate the role of SST (e.g., Barsugli and Battisti 1998). To evaluate the impact from these drawbacks, we analyzed the results of fully-forced 20-member historical AGCM simulations conducted by ESRL-CAM5 (available at www.esrl.noaa.gov/psd/repository

[/alias/facts/](#)), and also, 5-member historical (ALL) and natural (NAT) CMIP5 simulations conducted by MIROC5 (atmospheric components are exactly the same as the model used in this study). The linear trends of the historical simulations from 1958 to 2016 are 0.0569% per year of area fraction for the ALL-LNG run (Fig. 19.1c), 0.0590% per year for the ESRL-CAM5 AGCM simulations (Fig. ES19.2a), and 0.0764% per year for the coupled GCM of MIROC5 (Fig. ES19.2c). The sensitivity to different AGCM is relatively small between MIROC5 and CAM5 AGCMs. On the other hand, the difference between MIROC5 AGCM and CGCM suggests that the air–sea interaction might have some impacts on the occurrence of extreme warmth over Asia.

Conclusions. All of the risk of the extremely high temperatures over Asia in 2016 can be attributed to anthropogenic warming. In addition, the ENSO condition made the extreme warmth two times more likely to occur. It is found that anthropogenic warming contributed to raising the level of event probability almost everywhere, although the 2015/16 El Niño contributed to a regional increase of warm events over the Maritime Continent, the Philippines, and Southeast Asia, but had little significant contribution elsewhere in Asia.

ACKNOWLEDGMENTS. This work was supported by Grant-in-Aid 26247079, 26281013, 26800243, and the Program for Integrated Research Program for Advancing Climate Models (TOUGOU program) from the Ministry of Education, Culture, Sports, Science and Technology (MEXT), Japan.

REFERENCES

- Allen, M. R. 2003: Liability for climate change. *Nature*, **421**, 891–892, doi:10.1038/421891a.
- Barsugli, J. J., and D. S. Battisti, 1998: The basic effects of atmosphere–ocean thermal coupling on midlatitude variability. *J. Atmos. Sci.*, **55**, 477–493.
- Bellprat, O., and F. Doblas-Reyes, 2016: Attribution of extreme weather and climate events overestimated by unreliable climate simulations. *Geophys. Res. Lett.*, **43**, 2158–2164, doi:10.1002/2015GL067189.
- Christidis, N., and P. A. Stott, 2014: Change in the odds of warm years and seasons due to anthropogenic influence on the climate. *J. Climate*, **27**, 2607–2621, doi:10.1175/JCLI-D-13-00563.1.
- Gecker, J., and N. Chuwiruch, 2016: Thailand is used to hot Aprils, but not this hot! Bangkok AP news, Accessed 11 August 2017. [Available online at <https://apnews.com/42c7c080f86644168102ceeea105ddd0/thailand-used-hot-aprils-not-hot>].
- Hansen, J., R. Ruedy, M. Sato, and K. Lo, 2010: Global surface temperature change. *Rev. Geophys.*, **48**, RG4004, doi:10.1029/2010RG000345.
- Jones, G. S., P. A. Stott, and N. Christidis, 2008: Human contribution to rapidly increasing frequency of very warm Northern Hemisphere summers. *J. Geophys. Res.*, **113**, D02109, doi:10.1029/2007JD008914.
- Kimoto, M., and M. Ghil, 1993: Multiple flow regimes in the Northern Hemisphere winter. Part I: Methodology and hemispheric regimes. *J. Atmos. Sci.*, **50**, 2625–2643.
- Rayner, N. A., Parker, E. B. Horton, C. K. Folland, L. V. Alexander, D. P. Rowell, E. C. Kent, and A. Kaplan, 2003: Global analyses of sea surface temperature, sea ice, and night marine air temperature since the late nineteenth century. *J. Geophys. Res.*, **108**, 4407, doi:10.1029/2002JD002670.
- Shiogama, H., M. Watanabe, Y. Imada, M. Mori, Y. Kamae, M. Ishii, and M. Kimoto, 2014: Attribution of the June–July 2013 heat wave in the southwestern United States. *SOLA*, **10**, 122–126, doi:10.2151/sola.2014-025.
- , and Coauthors, 2016: Attributing historical changes in probabilities of record-breaking daily temperature and precipitation extreme events. *SOLA*, **12**, 225–231, doi:10.2151/sola.2016-045.
- Silverman, B. W., 1986: *Density Estimation for Statistics and Data Analysis*. Chapman and Hall, 175 pp.
- Stone, D. A., 2013: Boundary conditions for the C20C Detection and Attribution project: The ALL-Hist/est1 and NAT-Hist/CMIP5-est1 scenarios. International CLIVAR C20C+ Detection and Attribution Project, 18 pp. [Available online at http://portal.nersc.gov/c20c/input_data/C20C-DandA_dSSTs_All-Hist-est1_Nat-Hist-CMIP5-est1.pdf].
- Takahashi, C., M. Watanabe, H. Shiogama, Y. Imada, and M. Mori, 2016: A persistent Japanese heat wave in early August 2015: Roles of natural variability and human-induced warming [in “Explaining Extreme Events of 2015 from a Climate Perspective”]. *Bull. Amer. Meteor. Soc.*, **97** (12), S107–S112, doi:10.1175/BAMS-D-16-0157.1.
- Trenberth, K., J. M. Caron, D. P. Stepaniak, and S. Worley, 2002: Evolution of El Niño–Southern Oscillation and global atmospheric surface temperatures. *J. Geophys. Res.*, **107** (D8), doi:10.1029/2000JD000298.
- Watanabe, M., and Coauthors, 2010: Improved climate simulation by MIROC5: Mean states, variability, and climate sensitivity. *J. Climate*, **23**, 6312–6335, doi:10.1175/2010JCLI3679.1.
- Xie S.-P., K. Hu, J. Hafner, H. Tokinaga, Y. Du, G. Huang, and T. Sampe, 2009: Indian Ocean capacitor effect on Indo–western Pacific climate during the summer following El Niño. *J. Climate*, **22**, 730–747, doi:10.1175/2008JCLI2544.1.
- , Y. Kosaka, Y. Du, K. Hu, J. S. Chowdary, and G. Huang, 2016: Indo–western Pacific ocean capacitor and coherent climate anomalies in post-ENSO summer: A review. *Adv. Atmos. Sci.*, **33**, 411–432, doi:10.1007/s00376-015-5192-6.